Technologies and Materials for Renewable Energy, Environment & Sustainability

Enhancing Packaging Performance: A Thermal Study of Structural and Dielectric Behavior in Transparent Nylon

AIPCP25-CF-TMREES2025-00019 | Article

Enhancing Packaging Performance: A Thermal Study of Structural and Dielectric Behavior in Transparent Nylon

Riyam Abd Al-Zahra Fadil [1, a)], Salma Bassem Abdel Abbas [1, b),] Amel D. Hussein [2, c),] and Kareem Ali Jasim [3, d)]

[1] *Department of Physics, College of Science, Mustansiriyah University, Baghdad, Iraq 10052.*
[2] *College of Dentistry, University of Wasit, Wasit, Iraq 52001*
[3] *Department of Physics, College of Education for pure science, Ibn-Al-Haitham, University of Baghdad, Baghdad, Iraq 10001*

[a)] *Corresponding author* reyam_a24@uomustansiriyah.edu.iq
[b)] Salmaa.BA@uomustansiriyah.edu.iq
[c)] adashar@uowasit.edu.iq
[d)] kareem.a.j@ihcoedu.uobaghdad.edu.iq

ABSTRACT. In this paper, the structural properties of transparent nylon samples were studied using XRD analysis. Four samples were examined at different preparation temperatures: 130 °C, 150 °C, 170 °C, and 190 °C. The crystallite size was calculated using two methods: Williamson-Hall and Halder-Wagner. Amplitude (FWHM): 150 °C, (FWHM) was 0.26639 radians, indicating a larger amplitude. This shows the low content of impurities in the sample and the high degree of crystalline order. In the insulation properties test, there is a direct relationship between capacitance and temperature, while resistance and impedance exhibit nonlinear behavior and fluctuating values, but the relationship between inductance and temperature is inverse. **KEYWORDS.** Nylon, Polymer, Crystal Structure, UDM, Williamson Hall Method, Dielectric Properties.

INTRODUCTION

Nylon is a man-made material that has been applied in many industrial fields. Nylon has been studied for its ease, and many uses as an engineering plastic that can be easily converted into films, fibers, and molded parts. Nylon has desirable chemical stability and tunable mechanical properties, which make this material and its derivatives widely used as surgical sutures, catheters, dentures, etc., due to the biocompatible nature of this material (nylon) [1]. We knew that there were two main factors responsible for broadening the XRD peaks: lattice strain, crystal size, due to the large area of grain boundaries, and the imperfect nature of crystalline materials. Intrinsic strain of the crystal usually occurs [2], [3]. The reality of the volatility of ideal crystalline materials is due to the XRD peaks being broader, so we know that there is no perfect crystal due to its limited size. The width of the XRD peak is determined by the crystal size. Due to the appearance of polycrystalline aggregates, it is observed that the particle size and the size of the crystals are not the same [4], [5]. The low dielectric properties of polymeric materials are essential for high-speed signal transmission in high-frequency communications applications and microelectronic devices [6], [7]. Small changes in the water absorbed in a sample can cause significant changes in the electrical and dielectric properties of hygroscopic materials, meaning these properties are affected by the moisture content of biological materials [6]. The dielectric parameters, including inductance, conductivity, capacitance, and loss factor, were analyzed based on methodologies where LCR meter measurements under thermal variation were employed, similar to those of the research's [8], [9]. In this paper, transparent nylon for packaging will be studied and prepared practically to find the crystal size, use strain, and analyze the XRD result using the Origin 2019b 64Bit program with two methods of analysis, and Dielectric Properties.

THEORETICAL PART

(XRD) X-ray diffraction is the most important method for determining crystal structure and size in nanocrystals. To find the geometry of the particles, we use the XRD technique [10], [11], [12]. X-rays contributed to the study of this material, enabling the determination of its structural properties and interatomic spacing. The relationship and

influence between the structural properties of transparent nylon and temperature changes were also investigated.[13], [14]. Using (XRD), nylon samples are examined, and the distance (d_{hkl}) between the planes and the diffraction angle at the peak are calculated using Bragg's law [15], [16].

$$d = \frac{n\lambda}{2\ sin\ \theta} \quad (1)$$

Where d: Is distance (d_{hkl}) between levels and diffraction angle at the peak, λ: Wavelength of (XRD) used equal to 1.54060 Å. n: An order of integral numbers (1,2,…, etc.), θ: The angle of Bragg's between levels of atoms for crystals by Radians unit [17].

Williamson-Hall method

The Williamson-Hall(W-H) method is the easiest method used to find the crystalline size and strain. [18], [19]. Volume separation and strain expansion analysis were performed using the (W-H) difference, both of which are microscopic, due to the small crystal size and the microstrain resulting from the reflection amplitude depending on the different θ positions. It is a method that extends the Scherrer equation approach by taking into account the effects of microstrain in the crystal lattice. This is the basis of the W-H theory. The overall XRD broadening is assumed to be a combination of two factors: (i) strain broadening (due to lattice distortions in the material), and (ii) volume broadening (due to the finite crystal size).[20], [21].

Uniform Deformation Model (UDM)

In many cases, (XRD) patterns aren't affected just by the size of the crystals, but perhaps also by lattice defects and lattice strain. UDM stands for where it is supposed to stain uniformly in all crystallographic directions. βcosθ is plotted with respect to 4sinθ for the material peaks. The particle size is calculated from the slope and y-intercept of the straight-line equation. To measure crystallite size by UDM method, (XRD) can be used, shown in the equation below [20].

$$D_{UDM} = \left(\frac{K\lambda}{\beta\cos\theta}\right) + 4\,\varepsilon\,sin\theta \quad (1)$$

Where D_{UDM}: Crystallite size for ordered crystals. K: A factor approximately equal to (0.89-0.9 rad.$Å^{-2}$). λ: The x-ray wavelength in angstroms. β: The line broadening at (FWHM) peaks in Radian units. ε: The strain. θ: The angle of Bragg's in Radian units.

$$\text{The Crystallinity } (\delta) = \frac{\text{The Area of Crystalline Peaks}}{\text{Area of All Peaks}} * 100 \quad (3)$$

Halder – Wagner – Langford method

Advantage: more attention to the peaks of medium and low intensity, this method is very popular for finding the strain and size of a crystal simultaneously. The Halder–Wagner (H-W) method shows that the XRD reflectance isn't simply a Gaussian or Lorentzian function; Rather, it is a mixture of both. [22], [23], it follows the Lorentzian function with the following equations

$$\left(\frac{\beta^*}{d^*}\right)^2 = \left(\frac{k\beta^*}{\text{DHW}\ (d^{*2})}\right) + (2\,\varepsilon)^2 \quad (4)$$

After simplifying the equation, it becomes:

$$D_{HWL} = \left(\frac{k}{\beta^*}\right) + 4\,\varepsilon^2 \quad (5)$$

Where D_{HWL}: Is the crystallite size by Halder-Wagner, β^* : It is the broadening reciprocal lattice point, as equation below:

$$\beta^* = \frac{\beta\ cos\theta}{\lambda} \quad (6)$$

$$d = \frac{2\ sin\ \theta}{\lambda} \quad (7)$$

In tensile deformed specimens, the dislocation density (δ) increases linearly for a given stress, and this can be calculated from the equation below. UDM should also be suitable for calculating the lattice strain [24],[25], [26].

$$\delta = \frac{1}{D^2} \quad (8)$$

EXPERIMENTAL PART

Since impurities negatively affect the quality of the samples, the nylon used for packaging was thoroughly cleaned and prepared in the laboratory. The nylon was dissolved in formic acid after being cut into slim pieces. Nylon dissolution method: 5 grams of nylon were weighed and placed in a special tube. 550 milliliters of 70% formic acid were added. (Note: To obtain accurate results, samples were prepared in the summer in Iraq and at high temperatures.), We observed the nylon becoming more flexible and approaching a liquid state. Then we divided the quantity required into four samples to study the effect of temperature changes at four different temperatures. Put the first sample in oven at a temperature of (130), (150), (170), (190) °C, all for ten minutes. Then, four samples were scanned using XRD to study their structural properties, which were then examined at the SHIMADZU Laboratory. This is consistent with this research. [24]. After that, the dielectric properties of transparent nylon were investigated to assess the thermal influence on its electrical behavior. Inductance (L), capacitance (C), and dissipation factors (D) were measured using an HF LCR Meter 6500 Series device. Measurements were performed at a frequency of 100 Hz and a voltage of 10 mV, with the sample connected in parallel. This setup enabled accurate characterization of the dielectric response under different thermal conditions. According to this research [27].

RESULT AND DISCUSSION

(XRD) pattern for samples of nylon drawing between (2θ) in degree unit and intensity in arbitrary unit (a.u.), which shows that in all samples in one figure, there is a change in values of the peaks, as shown in Figure 1.

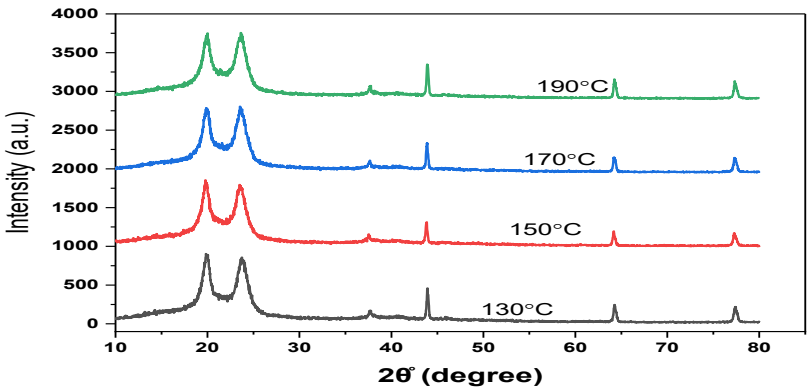

FIGURE 1. The XRD of Nylon.

Calculate Crystallinity, the area of all Peaks, and Area of Crystalline Peaks, for these samples at different temperatures. To calculate the average of FWHM in degrees and in radian units, after that, calculate the average of Interplanetary spacing in Angstrom units. As shown in Table 1.

Table (1) Values of crystallinity, Average of (β), (d), area of all Peaks, and area of crystalline Peaks in the fourth Temperature.

Temp. ℃	Crystallinity %	Avg. (FWHM=β) (radian)	Avg. Interplaner (d)	Area of all Peaks	Area of Crystalline Peaks
130℃	95.589	0.243246131	2.276207124	6526.84	6238.96
150℃	57.108	0.266394491	2.283260036	5933.88	3388.74
170℃	59.381	0.241872033	2.532272092	6199.12	3681.10
190℃	57.959	0.243098127	2.277942960	6303.34	3653.36

After calculating, crystallization was noted to have the highest percentage of crystallinity, 95.589%, at the lowest temperature, 130℃, used in this research. This means the rate of movement of atoms and molecules was acceptable, and they had sufficient time and temperature to reach organization and arrangement, which led to the formation of small crystalline or amorphous grains. Relationship between 4sinθ on X-axis and βCosθ on Y-axis in *Uniform Deformation Model,* and draw a better straight line by Origin 2019b program, and calculated crystallite size from slope of curve, as shown in Table 2, Figure 2.

Table (2) Crystallite size, dislocation Intensity, Intercept, and slope by UDM.

Uniform Deformation Model (UDM)				
Tem. ℃	**D (Å)**	**δ*10^{-5} (*lines* /Å^{-2})**	**Slope**	**Intercept**
130℃	132.194	5.72235	0.30026 ± 0.25044	-0.25973 ± 0.42008
150℃	119.987	6.94584	0.32956 ± 0.27165	-0.28527 ± 0.45553
170℃	140.015	5.10094	0.29927 ± 0.24685	-0.25988 ± 0.41440
190℃	143.344	4.86671	0.30030 ± 0.24943	-0.26019 ± 0.41857

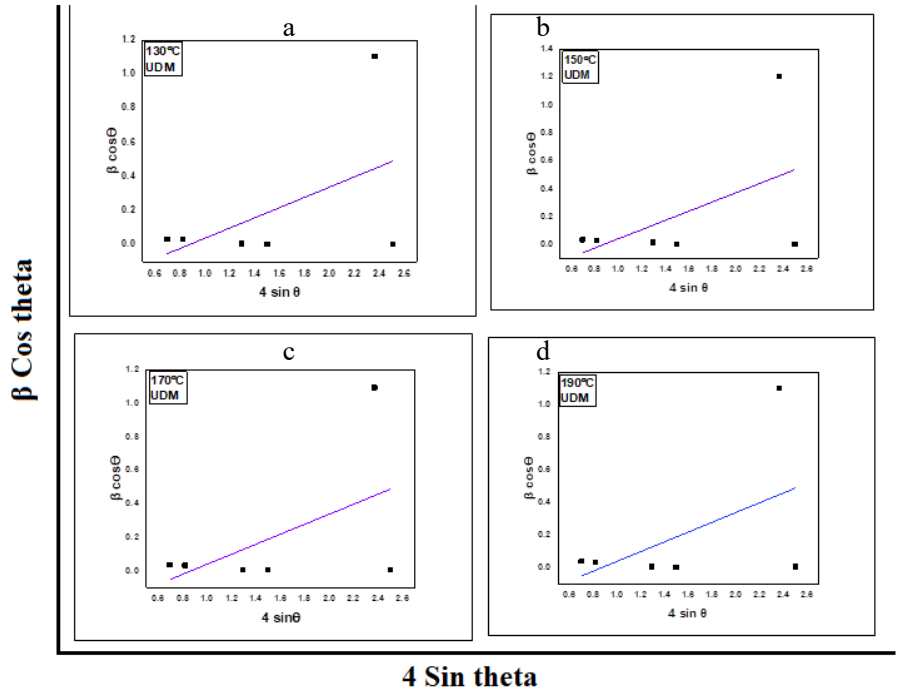

FIGURE 2a,b,c,d. Samples for Nylon using UDM.

Relationship between β^*/d^{*2} on X-axis, $(\beta^*/d^*)^2$ on Y-axis in Halder-Wagner Method, and draw the best straight line and calculate crystallite size from the slope of the curve, as shown in Table 3, Figure 3.

Table (3) Crystallite size, dislocation Intensity, Intercept, Slope by Halder-Wagner Method.

Halder-Wagner Method				
Tem. ℃	**D (Å)**	**δ*10^{-5} (*lines* /Å^{-2})**	**Intercept**	**Slope**
130℃	146.495	4.65965	-0.08872 ± 0.07959	0.69922 ± 0.14510
150℃	132.912	5.66066	-0.10879 ± 0.08867	0.77822 ± 0.14997
170℃	155.650	4.12760	-0.08571 ± 0.08187	0.68365 ± 0.15059
190℃	158.879	3.96153	-0.08582 ± 0.08394	0.68524 ± 0.15252

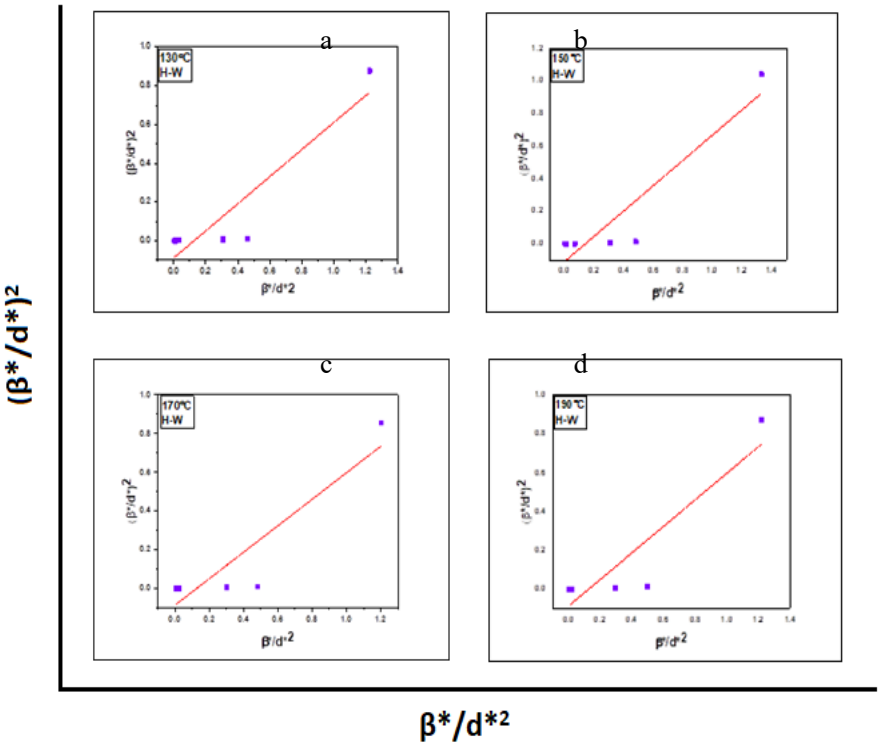

FIGURE 3a,b,c,d. Samples for nylon using the Halder-Wagner Method.

The dielectric properties of the transparent polymer film were studied over a wide temperature range to evaluate the material's behavior. Dielectric analysis is an important indicator for understanding a material's stability and efficiency in thermal and electronic applications. Capacitance (C), resistance (R), impedance (Z), and dielectric loss factors (tan δ) were measured using a suitable measuring device at increasing temperatures of (130, 150, 170, and 190) °C. The obtained values are shown in the table below and discussed later to explain the changes resulting from the thermal effect, as shown in Table 4.

Table (4) Dielectric values of nylon at different temperatures

Temp. T ℃	Capacitance C (PF)	Inductance L (KH)	Impedance Z (μΩ)	Resistance R (μΩ)	Dissipation Factor tanδ	Quality Factor Q
130℃	404.648	25.0393	5.09209	6.68067	1.17748	0.84927
150℃	547.747	18.4978	2.98318	3.47617	1.67174	0.59817
170℃	602.585	16.8144	5.21436	32.5908	0.16208	6.16968
190℃	933.214	10.8572	3.17957	8.78335	0.38833	2.57508

After calculating and measuring dielectric values at changing temperatures. We drew Relationship between Capacitance C in (PF) unit, Inductance L in (KH) unit, Impedance Z in (μΩ) unit and Resistance R in (μΩ) unit with changing temperature as shown in Fig. (4). We note that the capacity started at a low value compared to the low temperature for this research, and as the temperature increases, the capacity increases with it, this indicates an increase in the electrical insulation capacity of nylon as a result of thermal structural changes, i.e. there is a direct relationship between capacitance and temperature. As for inductance, the higher the temperature, the lower the inductance value. This indicates the effect of temperature on the internal structure of nylon, which affects its magnetic properties, i.e., the relationship is inverse [28]. The impedance and resistance showed non-linear behavior and fluctuated in value, sometimes rising and sometimes decreasing with increasing temperature, which indicates the presence of many irregular transition processes that affect the electrical and microscopic properties of Nylon [29].

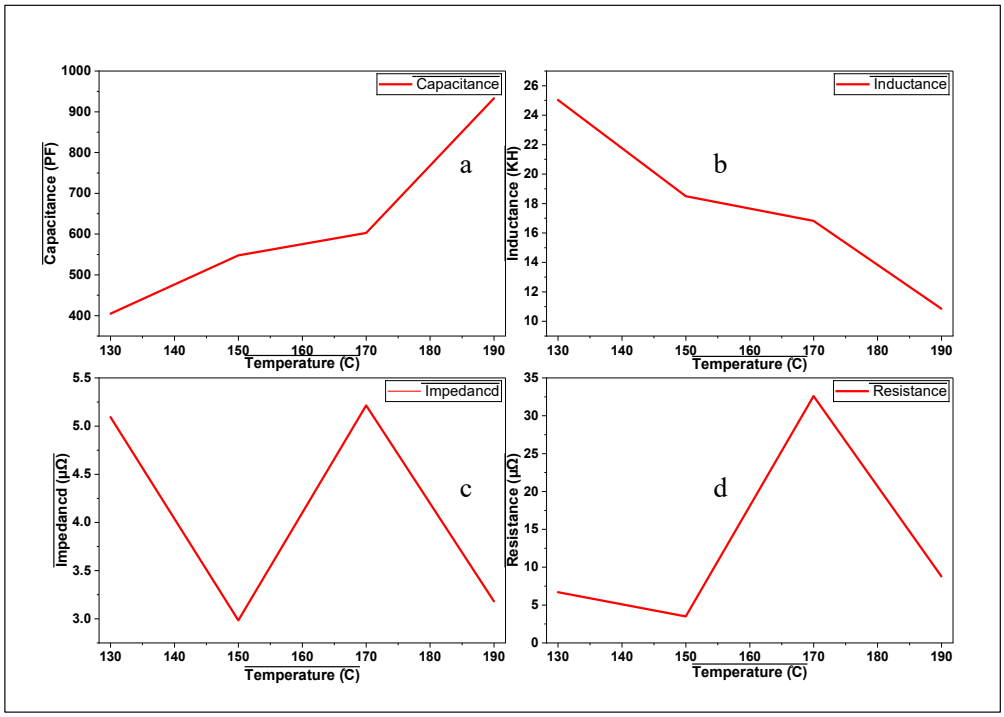

FIGURE 4a,b,c,d. Relationship between C, L, Z, and R with changing temperature.

Both the insulation loss factor and the quality factor were measured on the Y-axis versus the temperature on the X-axis. Figure (5) (A), (B) illustrates the results in the previous table, showing the inverse relationship between them, because the insulation loss factor started its movement at a temperature of 130°C, rose at 140°C, decreased until it reached a lower slope at 170°C, and then rose slightly at 190°C. The quality factor (Q) started at 130°C and decreased significantly, forming a slope at 140°C, then rose abruptly to reach its highest level at 170°C, and then declined at 190°C. This indicates the presence of a thermal transition point that affects the response and properties of the insulating material, leading to internal structural changes in the polymeric material, specifically the nylon material used in this paper.

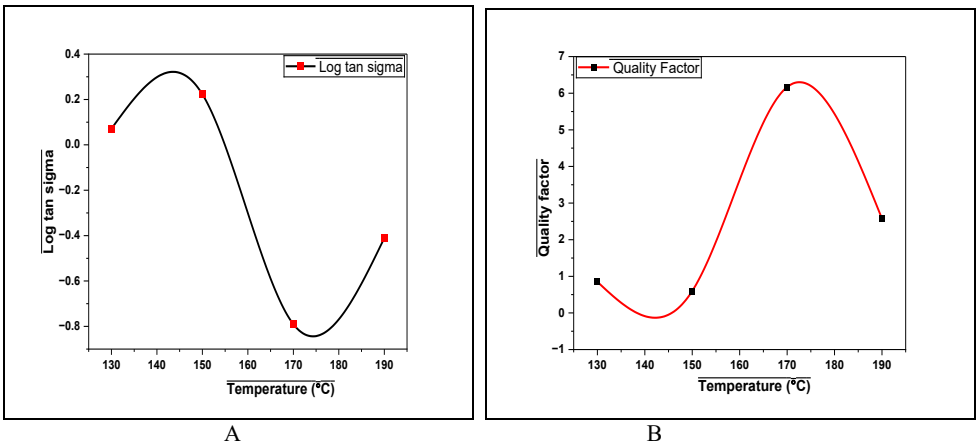

A B

FIGURE 5. (A) Relationship between tan insulation Dissipation factor with changing temperature. (B) Relationship between the Quality factor with changing temperature.

CONCLUSION

Transparent nylon samples were successfully synthesized in the laboratory using formic acid as a solvent. The samples underwent thermal sintering at four distinct temperatures, and their structural properties were investigated via XRD. The analysis revealed that temperature variations significantly influenced the (FWHM) values, calculated using Origin Pro 2019b software. Crystallite size was determined through both Halder-Wagner and Williamson-Hall methods. The Williamson-Hall approach allowed for peak broadening analysis, enabling the estimation of crystallite size and micro strain. The highest average crystallite size was recorded at 158.879 Å (Halder-Wagner) and 143.344 Å (UDM) at a sintering temperature of 190 °C. Interestingly, the highest crystallinity value of 95.589% was observed at 130 °C, indicating a non-linear relationship between temperature and crystallinity. Regarding the insulation properties, we observed a direct relationship between capacitance and temperature, and an inverse relationship between inductance and temperature. At the same time, resistance and impedance show nonlinear behavior.

FUTURE RECOMMENDATIONS

- Combining annealing with irradiation or plasma treatment and exploring how these treatments can affect crystallinity.
- Study the properties of nylon and relate the results to the medical and food industries.
- Study of the Optical and Mechanical properties of Nylon.

ACKNOWLEDGMENTS

The authors would like to thank Mustansiriyah University, Baghdad, Iraq, for its support in the present work. We also thank the Supervisor of the Superconducting Materials Laboratory / Department of Physics / College of Education for Pure Sciences-Ibn Al-Haitham / University of Baghdad for preparing the samples in the laboratory. We also thank Wasit University.

REFERENCES

1. M. Shakiba *et al.*, “Nylon—A material introduction and overview for biomedical applications,” *Polym. Adv. Technol.*, vol. 32, no. 9, pp. 3368–3383, 2021. https://doi.org/10.1002/pat.5372
2. G. S. Thool, A. K. Singh, R. S. Singh, A. Gupta, and M. A. B. H. Susan, “Facile synthesis of flat crystal ZnO thin films by solution growth method: A micro-structural investigation,” *J. Saudi Chem. Soc.*, vol. 18, no. 5, pp. 712–721, 2014. https://doi.org/10.1016/j.jscs.2014.02.005
3. R. Das and S. Sarkar, “X-ray diffraction analysis of synthesized silver nanohexagon for the study of their mechanical properties,” *Mater. Chem. Phys.*, vol. 167, pp. 97–102, 2015. https://doi.org/10.1016/j.matchemphys.2015.10.015
4. A. A. Akl and A. S. Hassanien, “Comparative microstructural studies using different methods: Effect of Cd-addition on crystallography, microstructural properties, and crystal imperfections of annealed nano-structural thin CdxZn1-xSe films,” *Phys. B Condens. Matter*, vol. 620, p. 413267, 2021. https://doi.org/10.1016/j.physb.2021.413267
5. R. Sivakami, S. Dhanuskodi, and R. Karvembu, “Estimation of lattice strain in nanocrystalline RuO2 by Williamson–Hall and size–strain plot methods,” *Spectrochim. Acta Part A Mol. Biomol. Spectrosc.*, vol. 152, pp. 43–50, 2016. https://doi.org/10.1016/j.saa.2015.07.008
6. K. Kardjilova, E. Bekov, Z. Hlavacova, and A. Kertezs, “Measurement of electrical properties of rapeseed seeds with LCR meter Good Will 8211,” *Int. J. Appl.*, vol. 2, no. 8, 2012.
7. M. R. Busireddy, L.-H. Meng, J.-W. Lin, W.-C. Ke, J.-T. Chen, and C.-S. Hsu, “Achieving Low Dissipation Factors and Low Dielectric Constants via Thermally Stable Naphthalene-Based Poly (ester-imide) s with Fluorine Groups,” *ACS Appl. Mater. Interfaces*, vol. 17, no. 12, pp. 18931–18939, 2025. https://doi.org/10.1021/acsami.5c00599
8. N. Mustafaeva, M. M. Asadov, A. I. Jabbarov, and E. M. Kerimova, “DIELECTRIC AND THERMOELECTRIC PROPERTIES OF CRYSTALS ON THE BASE OF TlInSe2–TlGaTe2 SYSTEM”.
9. H. Li *et al.*, “capacitance loss mechanism prediction based on electrochemical corrosion in metallized film capacitors,” *IEEE Trans. Dielectr. Electr. Insul.*, vol. 28, no. 2, pp. 654–662, 2021. https://doi.org/10.1109/TDEI.2020.009220

10. S. Bykkam, M. Ahmadipour, S. Narisngam, V. R. Kalagadda, and S. C. Chidurala, “Extensive studies on X-ray diffraction of green synthesized silver nanoparticles,” *Adv. Nanopart*, vol. 4, no. 1, pp. 1–10, 2015. DOI: 10.4236/anp.2015.41001
11. C. F. Holder and R. E. Schaak, “Tutorial on powder X-ray diffraction for characterizing nanoscale materials,” 2019, *ACS Publications*. https://doi.org/10.1021/acsnano.9b05157
12. J. Bardeen, L. N. Cooper, and J. R. Schrieffer, “Theory of superconductivity,” *Phys. Rev.*, vol. 108, no. 5, p. 1175, 1957. DOI: https://doi.org/10.1103/PhysRev.108.1175
13. O. V. Merkulov *et al.*, “Structural features and high-temperature transport in SrFe0. 7Mo0. 3O3− δ,” *J. Solid State Chem.*, vol. 258, pp. 447–452, 2018. https://doi.org/10.1016/j.jssc.2017.11.008
14. M. Julian and R. A. A.-Z. Fadil, “Effect of annealing temperatures on structural properties of Nylon,” in *Journal of Physics: Conference Series*, IOP Publishing, 2025, p. 12023. DOI 10.1088/1742-6596/3028/1/012023
15. F. R. A. Jasim.Kareem A, “Using XRD Analysis Methods by Modern Technical Programs to Study the Structural Properties of Hg1-xAgxBa2Ca2Cu3O8+d Compounds,” *AIP Conf. Proc.*, 2022. DOI: 10.1063/5.0092712
16. J. S. Mohammed *et al.*, “Investigate the structural properties of Tl1-xHgxSr2Ca2Cu3O8+ δ compound by using Scherrer modified equation,” in *AIP Conference Proceedings*, AIP Publishing, 2023. DOI: 10.1063/5.0129140
17. E. Parodi, G. W. M. Peters, and L. E. Govaert, “Structure-properties relations for polyamide 6, Part 2: Influence of processing conditions during injection moulding on deformation and failure kinetics,” *Polymers (Basel)*, vol. 10, no. 7, p. 779, 2018. https://doi.org/10.3390/polym10070779
18. M. Sakoda, K. Iida, and M. Naito, “Recent progress in thin-film growth of Fe-based superconductors: superior superconductivity achieved by thin films,” *Supercond. Sci. Technol.*, vol. 31, no. 9, p. 93001, 2018. DOI 10.1088/1361-6668/aabddb
19. H. Irfan, M. Racik K, and S. Anand, “Microstructural evaluation of CoAl2O4 nanoparticles by Williamson–Hall and size–strain plot methods,” *J. Asian Ceram. Soc.*, vol. 6, no. 1, pp. 54–62, 2018. https://doi.org/10.1080/21870764.2018.1439606
20. Y. Prabhu, K. V. Rao, V. S. S. Kumar, and B. S. Kumari, “X-ray analysis of Fe-doped ZnO nanoparticles by Williamson-Hall and size-strain plot methods,” *Int. J. Eng. Adv. Technol*, vol. 2, pp. 268–274, 2013.
21. Aleabi, S.H., Watan, A.W., Salman, E.M.-T., kareem Jasim A., Shaban, A.H., Alsaadi, T.M., The study effect of weight fraction on thermal and electrical conductivity for unsaturated polyester composite alone and hybrid, AIP Conference Proceedings, 2018, 1968, 020019.
22. Jasim, K.A., Alwan, T.J., Effect of Oxygen Treatment on the Structural and Electrical Properties of Tl0.85Cd0.15Sr2CuO5−δ, Tl0.85Cd0.15Sr2Ca2Cu2 O 7−δ and Tl0.85Cd0.15Sr3Ca2Cu3 O 9−δ Superconductors, Journal of Superconductivity and Novel Magnetism, 2017, 30(12), pp. 3451–3457.
23. R. A. A.-Z. Fadil, K. A. Jasim, and A. H. Shaban, “Sensitize the Electrical Properties of Partial Substitution on Mercury-Base Superconductor Manufactured By the Solid Reaction Method,” in AIP Conference Proceedings, 2022. doi: 10.1063/5.0092698.
24. R. A. F. Hamood, “Structural and Electrical Properties of Substitution elements on the Hg-base compound in High Temperature Superconductor,” University of Baghdad, 2021.
25. B. Himabindu, N. L. Devi, and B. R. Kanth, “Microstructural parameters from X-ray peak profile analysis by Williamson-Hall models; A review,” *Mater. Today Proc.*, vol. 47, pp. 4891–4896, 2021. https://doi.org/10.1016/j.matpr.2021.06.256
26. K. A. Jasim, R. A. A.-Z. Fadil, K. M. Wadi, and A. H. Shaban, “Partial Substitution of Copper with Nickel for the Superconducting Bismuth Compound and Its Effect on the Physical and Electrical Properties,” *Korean J. Mater. Res.*, vol. 33, no. 9, pp. 360–366, 2023, doi: 10.3740/MRSK.2023.33.9.360.
27. Saadon, A.K., Shaban, A.H., Jasim, K.A., Effects of the Ferrits addition on the properties of Polyethylene Terephthalate, Baghdad Science Journal, 2022, 19(1), pp. 208–216.
28. W. N. Alrefaei, F. M. Abd, and M. S. M. Al-jobori,,” *J. Pet. Res. Stud.*, vol. 7, no. 2, pp. 1–27, 2017. DOI: https://doi.org/10.52716/jprs.v7i2.178.
29. K. Al Abdullah, F. Al Alloush, A. Jaafar, and C. Salame, “Study of the effects related to the electric reverse stress currents on the mono-Si solar cell electrical parameters,” Energy Procedia 36, 104–113 (2013).